Available online at www.sciencedirect.com
SCIENCE DIRECT
Polymer 47 (2006) 3157–3163
polymer
www.elsevier.com/locate/polymer

Study of the kinetics of mushroom-to-brush transition of charged polymer chains

Guangming Liu, Lifeng Yan, Xi Chen, Guangzhao Zhang *

Hefei National Laboratory for Physical Sciences at Microscale, Department of Chemical Physics, University of Science and Technology of China, Hefei, Anhui 230026, China

Received 29 October 2005; received in revised form 21 February 2006; accepted 28 February 2006
Available online 23 March 2006

Abstract

The grafting of thiol-terminated poly[(2-dimethylamino)ethyl methacrylate] (HS-PDMEM) chains to a gold surface from a solution was investigated with quartz crystal microbalance with dissipation (QCM-D) in real time. The frequency and energy dissipation responses revealed a three-regime-kinetics of the grafting. The chains are quickly grafted in regime I forming a random mushroom. In regime II, the grafted chains have a rearrangement and form an ordered mushroom structure. The grafting is accelerated in regime III. As the grafting density increases, the chains form brushes. From regime II to III, the mushroom-to-brush transition occurs. The results were further supported by atomic force microscopy (AFM) imagines.

Keywords: Polymer brush; Kinetics of grafting; Quartz crystal microbalance

1. Introduction

It is well known that polymer chains grafted on a surface show much richer conformations than free chains because of the confinement of the chains near the surface [1–6]. At a low-grafting density, because the distance between grafting sites is larger than the size of the chains, the grafted polymer chains do not overlap. If the polymer segments have an attractive interaction with the surface, the polymer chains exhibit a so-called 'pancake-like' conformation. In contrast, if the segment–surface interaction is non-attractive, a 'mushroom' structure can be observed. At a high-grafting density, as the result of the balance between segment–segment repulsion and elasticity of the chains, the grafted chains are stretched away from the surface to form brushes, which is determined by the grafting density, structure of the chains, solvent quality and the segment–surface interaction. If the chains are charged, the conformations are dominated by the electrostatic interactions. Accordingly, the ionic strength and pH of the surrounding medium have great influence on the formation of the brushes [6].

So far most of the studies have been focused on the properties of the grafted chains in static equilibrium [7–16], both theoretical [17–21] and experimental [22–27] studies on the kinetics of grafting are limited. Theoretical investigations on kinetics of grafting predict two distinct regimes, i.e. the grafted chains form mushroom and brush structure in the first and second regime, respectively. However, Penn et al. [22] observed a three-regime-kinetics in recent experiments. It is apparent that the mechanism of such a grafting remains open.

Quartz crystal microbalance (QCM) has been used to study the adsorption, conformation and interactions of macromolecules in solution in real time [28–35]. On the other hand, gold surfaces have been used as a substrate for alkanethiol-based self-assembled monolayers (SAMs) because thiolate group can strongly interact with the gold surface with a bond strength about 40 kcal/mol [36–38]. A recent study revealed that the formation of such strong Au–S bonding was due to the restructuring of gold surface and incorporation of Au atoms into a growing 2D AuS phase induced by the adsorbed sulfur [39]. In the present study, we prepared narrowly-distributed thiol-terminated poly[(2-dimethylamino)ethyl methacrylate] (HS-PDMEM) with $pK_a = 6.6$ [40]. Such chains can be grafted on the gold surface of QCM sensor from an aqueous solution. Using QCM and atomic force microscopy (AFM), we investigated the kinetics of the grafting in situ. Our aim is to explore the mechanism of the formation of polymer brushes.

* Corresponding author. Tel./fax: +86 551 360 6763.
E-mail address: gzzhang@ustc.edu.cn (G. Zhang).

0032-3861/$ - see front matter © 2006 Elsevier Ltd. All rights reserved.
doi:10.1016/j.polymer.2006.02.091

2. Experiment section

2.1. Materials

2-(Dimethylamino)ethyl methacrylate (DMEM) (Aldrich) used as received. 4,4′-Azobis(isobutyronitrile) (AIBN) from Acros was purified by recrystallization from methanol. Tetrahydrofuran (THF) was distilled from a purple sodium benzophenone ketyl solution prior to use. Other regents were all used as received.

PDMEM terminated with dithioester (DTE-PDMEM) was synthesized by reversible addition fragmentation chain transfer (RAFT) polymerization [41]. The number-average molar mass (M_n = 21,858) and polydispersity index (M_w/M_n = 1.17) were determined by size exclusion chromatorgraphy (Waters 1515) using monodisperse polystyrene as standard and *N*,*N*-dimethylformamide (DMF) as eluent with a flow rate of 1.0 mL/min. The number-average molar mass determined by nuclear magnetic resonance (^{1}H NMR) is 21,153 g/mol.

DTE-PDMEM (20 mL, 2.35×10^{-3} g/mL) solution in water was mixed with 160 μL of 1.0 M $NaBH_4$ aqueous solution, and the mixture was stirred at room temperature for 1 week so that the dithioester groups were completely reduced into thiol groups [42].

2.2. Atomic force microscopy (AFM)

The polymer layer on the gold-coated crystal surfaces were imagined on an atomic force microscopy (AFM, Nanoscope IIIa, DI) in air. The root-mean-square (RMS) roughness of PDMEM layer was evaluated from the AFM images recorded [43]. To measure the thickness of the polymer layer, a small hole was first made by AFM scanning in contact mode so that the surface of substrate is exposed. Then, the topography in a large area was measured in tapping mode. The thickness was obtained by a section line analysis of the AFM height image. The thickness (h) of the layer in the final stage at pH 2, 6 and 10 were 3.8, 9.0 and 11.6 nm, respectively. From the number-average molar mass (M_n) of PDMEM chains, the thickness (h) and density ($\rho\sim1000$ kg/m^3) of the layer, the distance (d) between two anchoring sites can be evaluated using $d=(M_n/h\rho N_A)^{1/2}$. At pH 2, 6 and 10, d = 3.0, 2.0 and 1.7 nm, respectively. The radius of gyration (R_g) of PDMEM was evaluated to be 4.2 nm using $R_g = 0.26M_w^{1/2}$ [44,45]. Since, $2R_g > d$ at each pH, the grafted chains form brushes in the final stage.

2.3. QCM measurements

Quartz crystal microbalance with a dissipation monitoring (QCM-D) and the AT-cut quartz crystal with a fundamental resonant frequency of 5 MHz and a diameter of 14 mm were from Q-sense AB [46]. The quartz crystal was mounted in a fluid cell with one side exposed to the solution. The constant (C) of the crystal used was 17.7 ng/cm^2 Hz. The frequency shift was measurable to within ±1 Hz in aqueous medium.

When a quartz crystal is excited to oscillate in the thickness shear mode at its fundamental resonant frequency (f_0) by applying a RF voltage across the electrodes near the resonant frequency, a small layer added to the electrodes induces a decrease in resonant frequency (Δf) which is proportional to the mass (Δm) of the layer. In vacuum or air, if the added layer is rigid, evenly distributed and much thinner than the crystal, the Δf is related to Δm and the overtone number (n = 1, 3, 5,…) by the Sauerbrey equation [47]

$$\Delta m = -\frac{\rho_q l_q}{f_0}\frac{\Delta f}{n} \quad (1)$$

where f_0 is the fundamental frequency, ρ_q and l_q are the specific density and thickness of the quartz crystal, respectively. The dissipation factor (ΔD) is defined by $\Delta D = E_d/2\pi E_s$, where E_d is the energy dissipated during one oscillation and E_s is the energy stored in the oscillating system. The measurement of ΔD is based on the fact that the voltage over the crystal decays exponentially as a damped sinusoidal when the driving power of a piezoelectric oscillator is switched off [46]. By switching the driving voltage on and off periodically, we can simultaneously obtain a series of the changes of the resonant frequency and the dissipation factor. The solvent effect on the frequency and dissipation responses can be removed by using the corresponding solvent as the reference [48,49]. Since, the Sauerbrey equation might not be valid for the viscoelastic polymer layer, theoretical fitting based on a Voigt model was also done. Assuming that the layer is surrounded by a semi-infinite Newtonian fluid under no-slip condition and it has a uniform thickness, the changes of frequency (Δf) and dissipation (ΔD) were fitted by using a Q-tools software from Q-sense AB [50].

A measurement of grafting was initiated by switching the liquid exposed to the gold-coated quartz resonator from a pure solvent to a polymer solution with a concentration of 2.35×10^{-3} g/mL. Δf and ΔD values from the fundamental were usually noisy because of insufficient energy trapping and thus discarded [51]. In the present study, all experiments were conducted at 20 ± 0.02 °C.

3. Results and discussion

It is known that the polymer segment–surface interaction has heavy effects on the kinetics and mechanism of grafting. In the present study, the interaction between PDMEM segments and gold surface was examined by measuring the adsorption of DTE-PDMEM on the gold surface of QCM crystal. The only difference between DTE-PDMEM and HS-PDMEM is in the terminated group. Fig. 1 shows the frequency shift (Δf) of the quartz resonator relative to the aqueous solution as a function of time after DTE-PDMEM was introduced at different pH values. It can be seen $\Delta f\sim0$ at pH 6 and 2 after rinsing, indicating no segmental adsorption of DTE-PDMEM on the gold surface. Since, PDMEM has pK_a = 6.6, the chains are uncharged, partially charged and completely charged at pH 10, 6 and 2, respectively [40]. Obviously, the interaction between

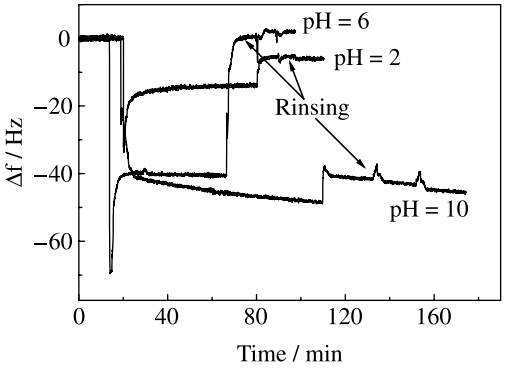

Fig. 1. Time dependence of frequency shift (Δf) of the quartz resonator immersed in DTE-PDMEM solution, where the overtone number (n) is 3.

the charged PDMEM segments and the gold surface is very weak. The fact also indicates that dithioester groups do not couple with gold. Note that the frequency shift before rinsing arises from the change of viscosity and density of the contacting medium. At pH 10, a small amount of DTE-PDMEM chains are adsorbed on the gold surface reflecting in $\Delta f \sim 43$ Hz after rinsing, indicating that there exists some interaction between the uncharged segments and the gold, but the interaction is not strong. Thus, PDMEM chains grafted on the gold surface are expected to form a mushroom structure instead of a pancake structure in the range at pH 2, 6 and 10.

Fig. 2 shows the changes of frequency (Δf) and dissipation (ΔD) of the quartz resonator immersed in an aqueous solution with pH 10 as a function of logarithmic time after HS-PDMEM was introduced. Note that either Δf or ΔD finally reaches a constant indicating the saturation of the gold surface. The changes in both Δf and ΔD indicate that the grafting has a three-regime-kinetics character. At the initial stage, the significant decrease in Δf (regime I) indicates that the chains quickly graft on the bare gold surface and the amount of grafting chains grow with time. Subsequently, the grafting slows down (regime II) because the grafting was hindered by the chains already grafted on the surface. Finally, the grafting speeds up reflecting in a relatively sharp decrease in Δf (regime III), indicating that the conformation of the already grafted chains has changed so that the incoming chains can be grafted on the surface. Parallelly, the dissipation change also gives the information about the structure of the polymer layer formed by the grafted chains. It is known that the dissipation of a viscoelastic polymer layer on quartz resonator increases with its thickness and looseness [50]. The quick increase in ΔD in regime I further indicates the grafting of the chains, whereas the slight increase in ΔD in regime II indicates that almost no grafting occurs. The large ΔD in regime III indicates a much thicker layer.

Figs. 3 and 4 show the changes of frequency (Δf) and dissipation (ΔD) at pH 6 and 2. Like the case in the uncharged chains at pH 10, the grafting of either partially or completely charged chains also have a three-regime-kinetics character. Such a three-regime-kinetics was first experimentally observed by Penn et al. [22] for the grafting of amine end-terminated polystyrene chains on the surface of silicate glass. This seems inconsistent with the previous theoretical studies where only two distinct regimes have been predicted [17–21]. In regime I, the grafting is controlled by the centre-of-mass diffusion of the chains from the solution, and the grafting density increases linearly with time until it reaches a certain critical value.

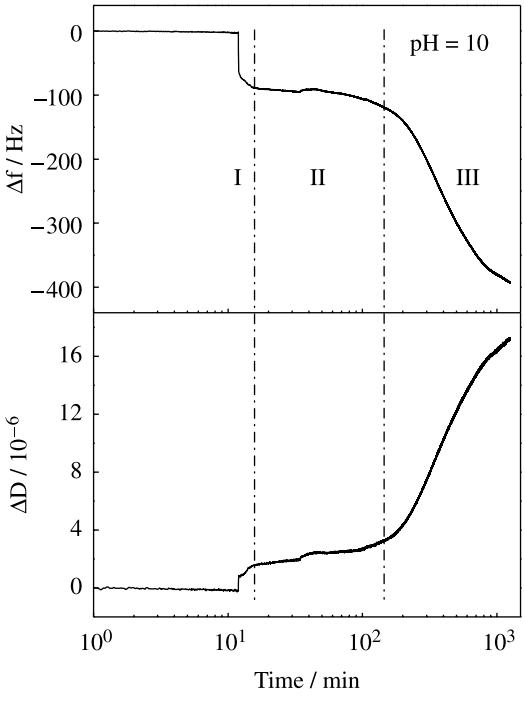

Fig. 2. The changes of frequency (Δf) and dissipation (ΔD) of the quartz resonator immersed in HS-PDMEM solution at pH 10 as a function of logarithmic time, where the overtone number (n) is 3.

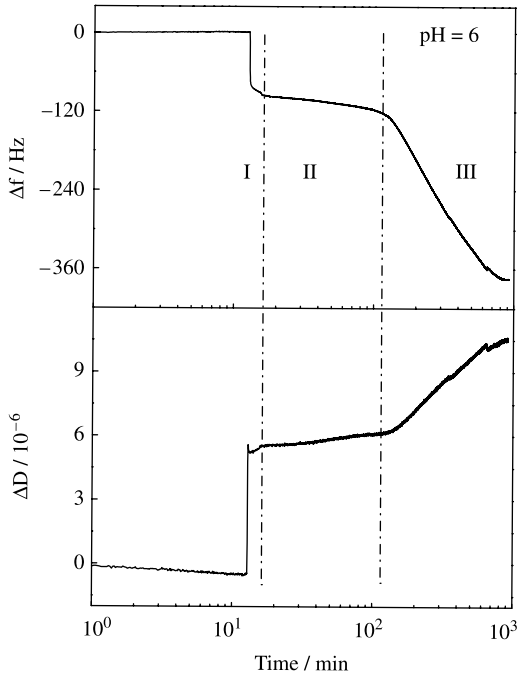

Fig. 3. The changes of frequency (Δf) and dissipation (ΔD) of the quartz resonator immersed in HS-PDMEM solution at pH 6 as a function of logarithmic time, where the overtone number (n) is 3.

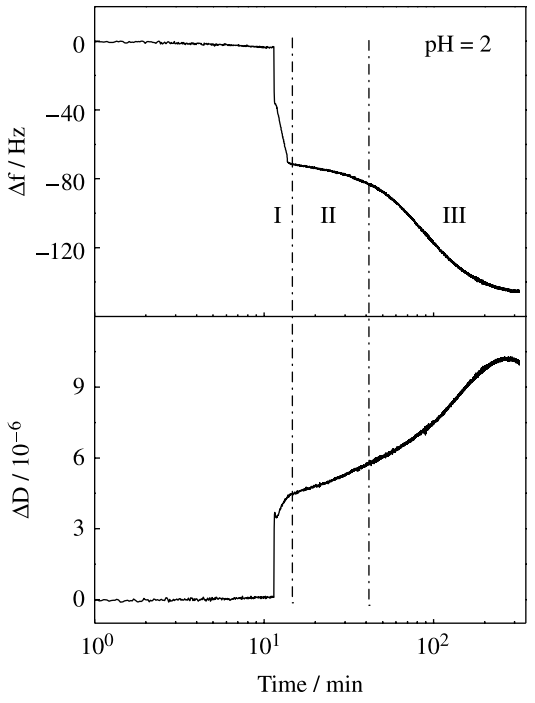

Fig. 4. The changes of frequency (Δf) and dissipation (ΔD) of the quartz resonator immersed in HS-PDMEM solution at pH 2 as a function of logarithmic time, where the overtone number (n) is 3.

In regime II, the grafting density increases slowly because the grafted chains create an energy barrier for further grafting. The grafting stops when the chains form stretched brushes. From regime II to III, the grafted chains undergo a mushroom-to-brush transition. Penn et al. [22] suggested that regime III observed in their experiments was not expected by theory, and the acceleration in regime III was attributed to the cooperative lateral contraction of incoming and grafted polymer chains. In order to understand such a three-regime-kinetics, the data in Figs. 2–4 has been carefully analyzed.

Figs. 2–4 show that the span for regime II has much dependence on the degree of charging of the grafted chains. It covers ~130 min at pH 10 (Fig. 2), but it drops to ~90 min when the chains are partially charged at pH 6. The complete charging at pH 2 leads regime II to be only ~30 min. As discussed above, the grafting is very slow in regime II reflecting in the slight changes in Δf and ΔD. What happens in regime II is the rearrangement of the chains. Figs. 2–4 clearly show that the time for the rearrangement decreases with the degree of charging. In other words, highly charged chains can easily rearrange themselves. However, why does such a rearrangement occur in regime II? It is known that the chains are quickly grafted in regime I. Such a grafting, which is controlled by the centre-of-mass diffusion of the chains, leads the chains to be randomly tethered on the gold surface, and some 'local' overlapping of the chains is resulted. Obviously, the locally overlapped chains are in a non-equilibrium state. Driven by the balance between the local segment–segment repulsion and elasticity of the chains, the chains tend to eliminate the local overlapping, and thus make a rearrangement themselves. As the degree of charging increases, the electrostatic repulsion between the chains becomes strong, and the chains tended to be stretched with a small tube diameter [52] (Scheme 1), which leads the local overlapping to be more difficult. That's why the time for the rearrangement decreases with the degree of charging. Besides, the interaction between the already grafted chains and the incoming chains might also influence the rearrangement [22]. In short, our results indicate that conformation of the grafted chains in regime II is slightly different from that in regime I, i.e. the chains form a 'random' mushroom in regime I but a 'ordered' mushroom in regime II. The latter without local overlapping of chains makes further grafting possible. After the rearrangement, the space between two neighbor chains is enough to accommodate incoming chains.

In regime III, the grafting through the ordered mushroom structure progresses until saturation is reached. The marked changes in frequency and dissipation from regime II to III suggest that the grafted chains form a structure much different from the mushroom structure in regime I and II, or the chains

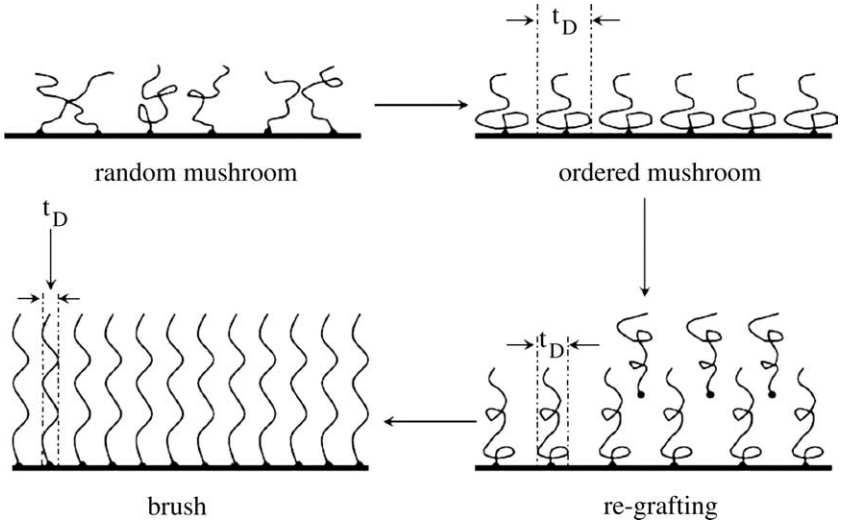

Scheme 1. Grafting of HS-PDMEM chains on gold surface.

should form brushes in regime III. The gradual decrease in Δf and increase in ΔD with time in regime III indicate that the grafting density increases and the chains become stretching. Note that both the frequency shift (Δf_s) and dissipation factor (ΔD_s) at saturation decrease with the degree of charging. This is understandable. Due to the electrostatic repulsion, an incoming chain must keep its distance from an already grafted chain so that it can be grafted. A strong repulsion leads to a large distance or a small grafting density. Accordingly, Δf_s and ΔD_s decrease with the degree of charging. The grafting kinetics can be better viewed in terms of ΔD vs Δf relation in Fig. 5.

ΔD vs Δf relation has proven useful for studying conformational changes of macromolecules [30,53]. Fig. 5 shows that for either uncharged, partially charged chains or completely charged chains, the grafting involves two kinds of kinetic processes. Regime I and II have the same ΔD vs Δf relation, clearly indicating only a minor difference between the conformations of the chains in the two regimes, or the chains form a mushroom structure in both regime I and II. In regime III, a quite different kinetic process can be observed, indicating that the grafted chains in this regime have a conformation different from that in regime I and II, i.e. they form brushes. Accordingly, from regime II to III, the mushroom-to-brush transition occurs.

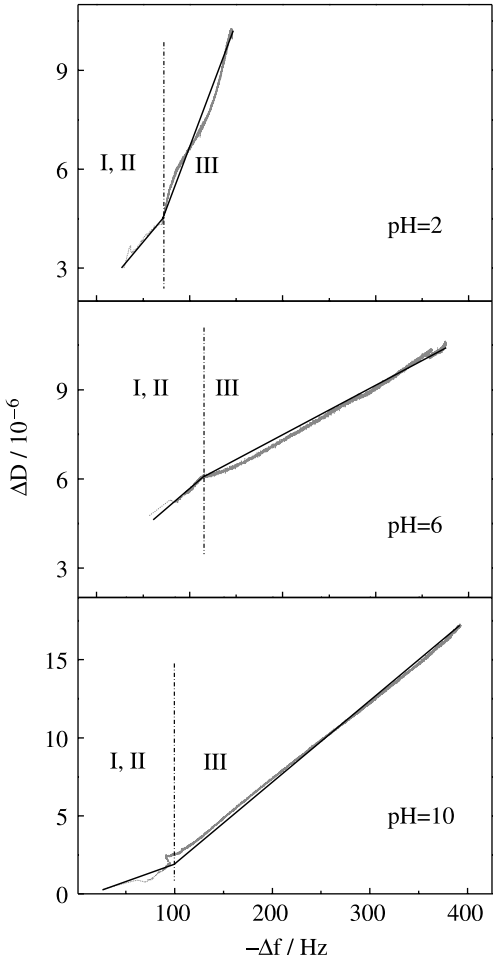

Fig. 5. Plot of ΔD vs Δf relation of HS-PDMEM layer at pH 2, 6 and 10, where the overtone number (n) is 3.

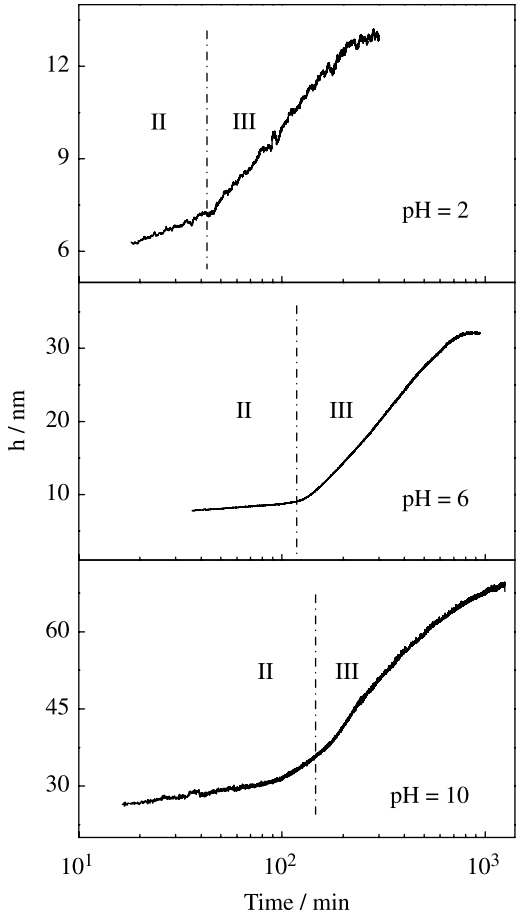

Fig. 6. The time dependence of the hydrodynamic thickness of the HS-PDMEM layer at pH 2, 6 and 10 fitted using Voigt model.

Fig. 6 shows the time dependence of hydrodynamic thickness (h) of the HS-PDMEM layer fitted based on Voigt model for the frequency change (Δf) at $n=3$, 5, 7. As the bulk solution is dilute, its density (ρ_l) and viscosity (η_l) were assumed to be close to those of water, i.e. $\rho_l \sim 1000\ \mathrm{kg/m^{-3}}$ and $\eta_l \sim 1\times10^{-3}$ Pa s, respectively. The density (ρ_f) of the adsorbed layer used was $\sim 1000\ \mathrm{kg/m^{-3}}$. Note that the results can be compared relatively to each other though the absolute values might be overestimated due to the over-simplification of the model. The fitting in regime I was not

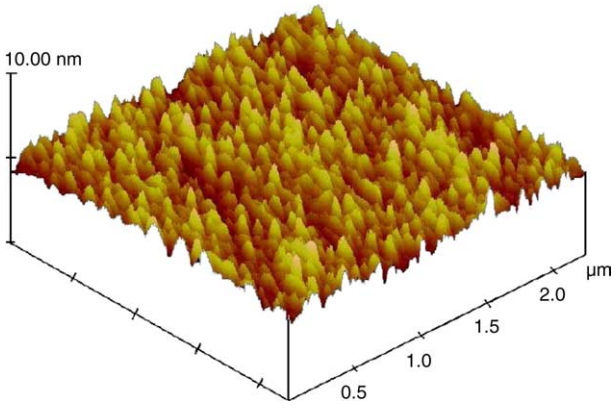

Fig. 7. The AFM image of the bare gold-coated crystal surface.

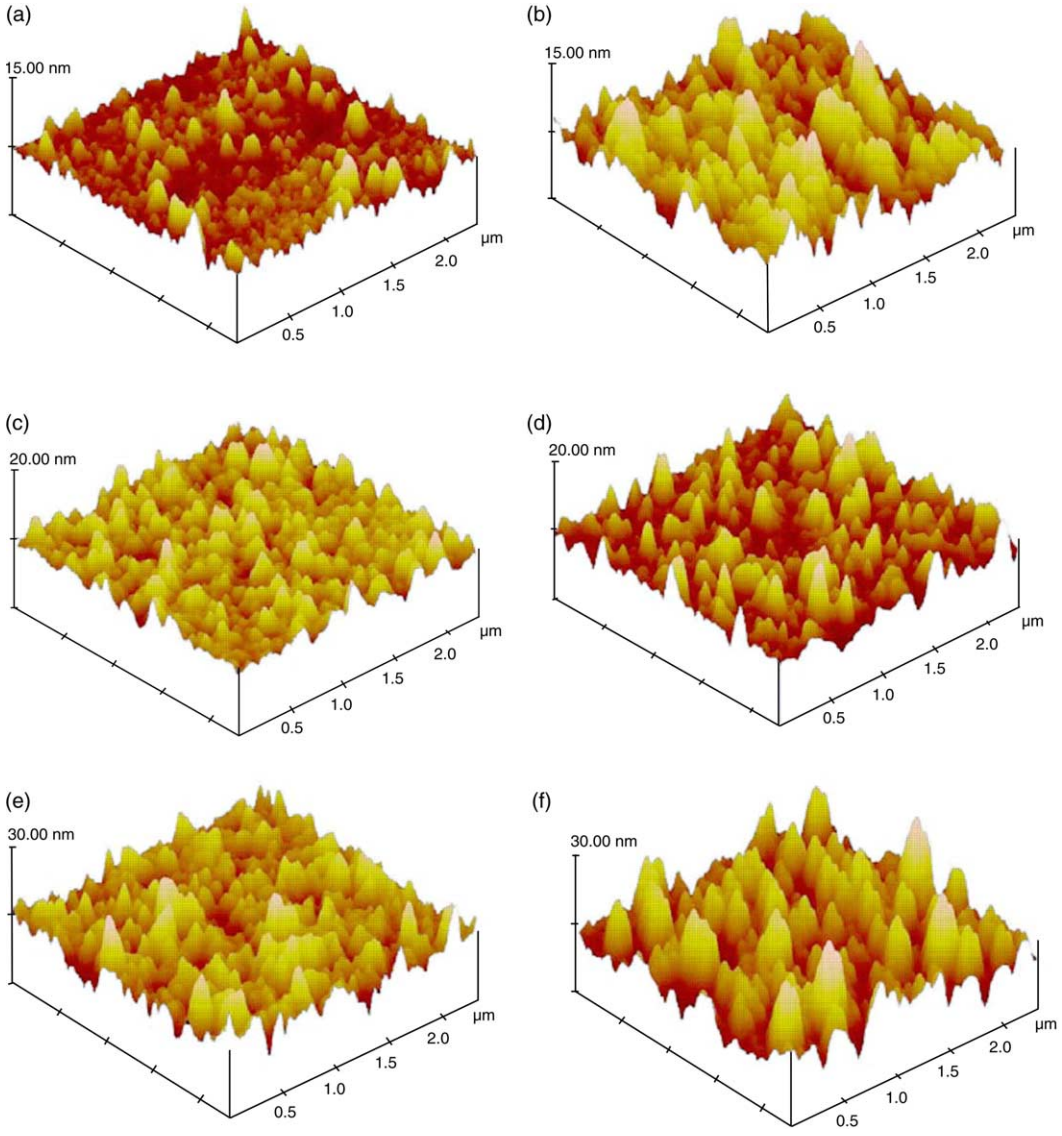

Fig. 8. AFM images of PDMEM layers at different pH: (a) in regime II at pH 2; (b) in regime III at pH 2; (c) in regime II at pH 6; (d) in regime III at pH 6; (e) in regime II at pH 10; (f) in regime III at pH 10.

done since the Voigt model does not suit for such a situation where pure solvent is quickly replaced by the polymer solution. In regime II, the hydrodynamic thickness slightly increases at each pH, further indicating that a rearrangement occurs leading the grafted chains to be more extended, i.e. the layer transits from a random mushroom to an ordered mushroom. The fact that the hydrodynamic thickness in regime III is larger than that in regime II indicates the stretching of the grafted chains. A similar behavior has also been observed by Genzer et al. for poly(acrylamide) brushes [54]. The turn between regime II and III indicates the occurrence of mushroom-to-brush transition there. The increase in h in regime III indicates that the brushes tend to be more stretched with the increasing grafting density. Our results show that regime II instead of regime III [22] is beyond the theoretical prediction [17–21], this is because the rearrangement of the chains was not taken into consideration in the theoretical studies.

The structures of polymer layer formed in regime II and III were also examined by AFM. Fig. 7 shows the AFM image of the bare gold crystal surface before grafting. It can be seen that the surface is very smooth with RMS roughness ~0.75 nm. Fig. 8(a) and (b) are the topographical images of PDMEM layer in regime II (~40 min) and regime III (~310 min) at pH 2. The RMS roughness values are ~1.47 and ~2.80 nm, respectively. At pH 6 (Fig. 8(c) and (d)), the RMS roughness value increases from ~2.00 nm in region II (~70 min) to 2.95 nm in region III (~850 min). At pH 10 (Fig. 8(e) and (f)), the RMS roughness values in regime II (~100 min) and regime III (~1250 min) are ~4.83 and 8.10 nm, respectively. As we mentioned in the experimental section, the chains form brushes in the final stage. Obviously, a higher degree of charging leads to a more stretched brush. Since, the roughness increases with the stretching of the chains, the fact that the roughness increases from regime II to III at each pH implies that the mushroom-to-brush transition occurs there. The mechanism of the grafting is described in Scheme 1.

4. Conclusion

In conclusion, we have investigated the grafting of thiol-terminated poly[(2-dimethylamino)ethyl methacrylate] (HS-PDMEM) chains to gold surface from a solution with quartz crystal microbalance (QCM) and atomic force microscopy (AFM). Our studies reveal a three-regime-kinetics of the grafting. HS-PDMEM chains form a random mushroom in regime I. In regime II, the chains rearrange themselves to eliminate the local overlapping and form an ordered mushroom. In regime III, the chains form brushes. The mushroom-to-brush occurs in the region from regime II to III. The tube diameter of the chain depending on the degree of charging is an important parameter for the grafting. As pH decreases, the degree of charging increases, leading the tube diameter to decrease, so that the time for the rearrangement of the chains decreases.

Acknowledgements

The financial support of the National Major Research Plan Projects (90303021) is gratefully acknowledged.

References

[1] Alexander S. J Phys (Fr) 1977;38:983.
[2] de Gennes PG. Macromolecules 1980;13:1069.
[3] Milner ST. Science 1991;251:905.
[4] Halperin A, Tirrell M, Lodge TP. Adv Polym Sci 1991;100:31.
[5] Zhao B, Brittain WJ. Prog Polym Sci 2000;25:677.
[6] Rühe J, Ballauff M, Biesalski M, Dziezok P, Gröhn F, Johannsmann D, et al. Adv Polym Sci 2004;165:79.
[7] Kritikos G, Terzis F. Polymer 2005;46:8355.
[8] Hu DJ, Cheng ZP, Zhu J, Zhu XL. Polymer 2005;46:7563.
[9] Zhao B, Haasch RT, MacLaren S. J Am Chem Soc 2004;126:6124.
[10] Manciu M, Ruckenstein E. Langmuir 2004;20:6490.
[11] Kizhakkedathu JN, Kumar KR, Goodman D, Brooks DE. Polymer 2004;45:7471.
[12] Park JW, Thomas EL. J Am Chem Soc 2002;124:514.
[13] Zhao HY, Farrell BP, Shipp DA. Polymer 2004;45:4473.
[14] Terzis AF. Polymer 2002;43:2435.
[15] Karim A, Satija SK, Douglas JF, Ankner JF, Fetters LJ. Phys Rev Lett 1994;73:3407.
[16] Romet-Lemonne G, Daillant J, Guenoun P, Yang J, Mays JW. Phys Rev Lett 2004;93:148301.
[17] Ligoure C, Leibler L. J Phys (Paris) 1990;51:1313.
[18] Hasegawa R, Doi M. Macromolecules 1997;30:5490.
[19] Fredrickson GH, Milner ST. Macromolecules 1996;29:7386.
[20] O'Shaughnessy B, Sawhney U. Macromolecules 1996;29:7230.
[21] Kramer EJ. Isr J Chem 1995;35:49.
[22] (a) Penn LS, Hunter TF, Lee Y, Quirk RP. Macromolecules 2000;33:1105.
(b) Penn LS, Huang H, Sindkhedkar MD, Rankin SE, Chittenden K, Quirk RP, et al. Macromolecules 2002;35:7054.
(c) Huang H, Penn LS, Quirk RP, Cheong TH. Macromolecules 2004;37:516.
(d) Huang H, Penn LS, Quirk RP, Cheong TH. Macromolecules 2004;37:5807.
(e) Huang H, Rankin SE, Penn LS, Quirk RP, Cheong TH. Langmuir 2004;20:5770.
[23] (a) Himmelhaus M, Bastuck T, Tokumitsu S, Grunze M, Livadaru L, Kreuzer HJ. Europhys Lett 2003;64:378.
(b) Tokumitsu S, Liebich A, Herrwerth S, Eck W, Himmelhaus M, Grunze M. Langmuir 2002;18:8862.
[24] (a) Stamm M, Motschmann H, Toprakcioglu C. Macromolecules 1991;24:3681.
(b) Dorgan JR, Stamm M, Draper J, Toprakcioglu C, Jérôme R, Fetters LJ. Macromolecules 1993;26:5321.
(c) Luzinov I, Minko S, Tokarev I, Stamm M. Langmuir 2004;20:4064.
[25] Abraham T, Giasson S, Gohy JF, Jérôme R, Müller B, Stamm M. Macromolecules 2000;33:6051.
[26] Huguenard C, Varoqui R, Pefferkorn E. Macromolecules 1991;24:2226.
[27] Tao J, Guo A, Stewart S, Birss VI, Liu G. Macromolecules 1998;31:172.
[28] Plunkett MA, Wang ZH, Rutland MW, Johannsmann D. Langmuir 2003;19:6837.
[29] Domack A, Prucker S, Rühe J, Johannsmann D. Phys Rev E 1997;56:680.
[30] Höök F, Rodahl M, Brezinski P, Kasemo B, Brezinski P. Proc Natl Acad Sci USA 1998;95:12271.
[31] Munro JC, Frank CW. Macromolecules 2004;37:925.
[32] Fu TZ, Stimming U, Durning CJ. Macromolecules 1993;26:3271.
[33] Xu H, Schlenoff JB. Langmuir 1994;10:241.
[34] Ivanchenko MI, Kobayashi H, Eduard AK, Dobrova NB. Anal Chim Acta 1995;314:23.
[35] (a) Moya S, Azzaroni O, Farhan T, Osborne VL, Huck WTS. Angew Chem, Int Ed 2005;44:4578.
(b) Azzaroni O, Moya S, Farhan T, Brown AA, Huck WTS. Macromolecules 2005;38:10192.
(c) Moya S, Brown AA, Azzaroni O, Huck WTS. Macromol Rapid Commun 2005;26:1117.
[36] Poirier GE. Chem Rev 1997;97:1117.
[37] Ulman A. Chem Rev 1996;96:1533.
[38] Love JC, Estroff LA, Kriebel JK, Nuzzo RG, Whitesides GM. Chem Rev 2005;105:1103.
[39] Biener MM, Biener J, Friend CM. Langmuir 2005;21:1668.
[40] Lee AS, Gast AP, Bütün V, Armes SP. Macromolecules 1999;32:4302.
[41] (a) Thang SH, Chong YK, Mayadunne RTA, Moad G, Rizzardo E. Tetrahedron Lett 1999;40:2435.
(b) Goto A, Sato K, Tsujii Y, Fukuda T, Moad G, Rizzardo E, et al. Macromolecules 2001;34:402.
[42] Zhu MQ, Wang LQ, Exarhos GJ, Li ADQ. J Am Chem Soc 2004;126:2656.
[43] Xu S, Arnsdorf MF. J Microsc 1994;173:199.
[44] Wesley RD, Cosgrove T, Thompson L, Armes SP, Baines FL. Langmuir 2002;18:5704.
[45] O'Reilly JM, Teegarden DM, Wignall GD. Macromolecules 1985;18:2747.
[46] Rodahl M, Höök F, Krozer A, Kasemo B, Breszinsky P. Rev Sci Instrum 1995;66:3924.
[47] Sauerbrey G. Z Phys 1959;155:206.
[48] Kanazawa KZ, Gordon III JG. Anal Chem 1985;57:1770.
[49] (a) Stockbridge CD. In: Katz MJ, editor. Vacuum microbalance techniques. New York: Plenum Press; 1966.
(b) Rodahl M, Kasemo B. Sens Actuators A 1996;54:448.
[50] Voinova MV, Rodahl M, Jonson M, Kasemo B. Phys Scr 1999;59:391.
[51] Bottom VE. Introduction to quartz crystal unit design. New York: Van Nostrand Reinhold Co.; 1982.
[52] de Gennes PG. Scalling concepts in polymer dynamics. Ithaca, NY: Cornell University Press; 1979.
[53] (a) Liu GM, Zhang GZ. J Phys Chem B 2005;109:743.
(b) Liu GM, Zhang GZ. Langmuir 2005;21:2086.
[54] (a) Wu T, Efimenko K, Genzer J. J Am Chem Soc 2002;124:9394.
(b) Wu T, Efimenko K, Vlček P, Šubr V, Genzer J. Macromolecules 2003;36:2448.